Shashi Chichkhede
Ph.D. scholar
National institute of technology, Raipur (C.G)
Mechanical engineering department,
India

Deepak Mahapatra
Assistant Professor
Indira Gandhi Krishi Vishwavidyalaya, Raipur (C.G)
Agricultural engineering department,
India

Shubhashis Sanyal
Professor
National institute of technology, Raipur (C.G)
Mechanical engineering department,
India

Shubhankar Bhowmick
Associate Professor
National institute of technology, Raipur (C.G)
Mechanical engineering department,
India

Static Behaviour of Functionally Graded Rotating Cantilever Beams Using B-Spline Collocation Technique

The present work reports the static behaviour of functionally graded rotating beam based on Timoshenko beam theory, which includes the effect of shear deformation. The principle of virtual displacement is applied to derive a governing equation for the functionally graded (FG) rotating beam, considering the centrifugal stiffening effect. The B-spline collocation technique is employed to solve the differential equation and material properties are function of power law distribution. The effect of material power index and rotational speed on the static characteristics of functionally graded rotating cantilever beams has been investigated for two different slenderness ratios. The obtained results demonstrate the beam deflection and the beam normal and shear stresses for the power gradient and rotational speed values. The results help to conclude that material gradation can be utilized to improve the functioning of the rotating structures such as helicopter rotor, aircraft propellers, windmill blades etc.

Keywords: *functionally graded material; rotating beam; B-spline collocation method; static behaviour; stress and deformation analysis*

1. INTRODUCTION

Functionally graded materials are a new class under composites where the material constituent is tailored in a way to give a gradual variation of material properties, thus, avoiding failure due to interfacial stress con–centration, delamination, and cracking of the matrix as commonly found in composites. Due to superior pro–perties, a functionally graded material finds wide range of applications in structures. Rotating beams are often used to model structural elements such as helicopter blades, airplane propellers, windmill rotors, and other blades of turbomachinery. The authors in paper [1] have described the unpredictable failure of the composite material of helicopter blade under influence of various force. The authors [2], have studied helicopter blades to investigate damage growth in material that resulted in matrix cracking, debonding/delamination, and fibre breakage using the finite element method.

In their paper [3], authors have conducted a case study of a military helicopter crash that indicated failure in blade due to the fatigue mechanism caused by an incision made during spar maintenance. Therefore, it becomes necessary to evaluate the material of the rota–ting structure to avoid accumulation. of stresses, crac–king and debonding of material caused due to damage of the component.

The study of Euler-Bernoulli beams was done by the rational interpolation functions to solve governing differential equation for Euler–Bernoulli rotating beam to analyse static and dynamic behaviour for homo–genous material. A modified Gazelle helicopter blade has been analysed to study the natural frequency and mode shape by [5] using Lanczos method to extract decomposition matrix and eigenvalue. [6]also developed new beam element to analysis the behaviour of func–tionally graded material for a beam structure, where static and free vibration analysis of functionally graded material (FGM) beam under thermal loading was done. Early work reported by [7] and [8] focussed on formulating a decoupled equation of motion based on Timoshenko beam theory. Where using a power series solution to evaluate the dynamic characteristic of a rotating isotropic beam.

The work by [9] has considered the effect of Coriolis force on natural frequency of rotating beam, [10] has investigated flap-wise bending vibration along with coupled lag-wise bending and axial vibration to study the effect of Coriolis force, slenderness ratio at high angular velocity using power series solution. [11] approached through the finite element method to analysis natural frequency, time responses, and distri–butions of deformation and stresses for functionally graded rotating beam. Similarly, [12] also used the finite element method to study a nonlinear rotating beam model which considers the effect of geometric stiffness, Coriolis force applied to isotropic, composite, and func–tionally graded beam. Early studies on rotating beam have ignored the term $\rho I\Omega^2\theta$, [13] has identified the significance of this term at higher speed. In paper [14] the authors have studied free vibration of the Timos–henko beam using a differential transform method to examine various geometrical parameters on vibrational characteristics of rotating FG beam. The study by [15] analysed free vibration of a tapered rotating beam using the frobenius method of series solution. In another article by [16], introduced NURBS-based finite element

Received: Decmeber 2022, Accepted: May 2023
Correspondence to: Dr Shubhankar Bhowmick,
Associate Professor, National institute of technology,
Raipur (C.G), India
E-mail: sbhwomick.mech@nitrr.ac.in
doi: 10.5937/fme2303347C

formulation to investigate flap-wise vibration. [17], in their work, have analysed stress distribution and defor–mation of a functionally graded beam using the B-spline collocation method. In this paper, [18] the authors have investigated the effect of tapering on a rotating beam. [19] solved the differential equation using spectral finite element method to analysis mode shape and modal frequency for uniformly tapered rotating beam.

In their widely acclaimed work by [20], the authors have derived a single fourth order governing partial differential equation for static and dynamic analysis of non-rotating beam. Euler–Bernoulli and Timoshenko beam theory was used to study deflection and stress distribution in functionally graded material. Wave pro–pagation and free vibration was studied for dynamic analysis. Results reported by [21] suggest that the derived flexural stiffness function of a rotating beam whose eigen pair is equivalent to a non-rotating beam can be employed to check the code and develop the actual beam to counter the stiffening effect due to the centrifugal force. [22] as compared two methods, that is, the differential transformation method (DTM) and the differential quadrature element method, to analyse the free vibration of FG tapered rotating beam. For various boundary conditions, [23] studied free vibration of axially functionally graded nonuniform cross-section beam using Fredholm integral equations. In paper [24] the authors have used the ANSYS workbench to study the static and dynamic characteristics of functionally graded material. A recent analysis by [25] highlights stress and vibration analysis for a functionally graded rotating beam where the effect of material gradation and rotation speed has been studied. [26] has investigated bending deformation and vibration behaviour of functionally graded rotating beam using novel floating frame reference (FFR) formulation. [27] has inves–tigated non-linear behaviour of rotating beam at large amplitude where hardening /softening effect at various rotating speed has been analysed. Axially graded non-uniform beam was investigated by [28] for wrinkle type of elastic foundation, where using energy method dynamic analysis was done on FG beam. Using the Rayleigh-Ritz method coupled with Kane's method [29] has studied vibration characteristics of rotating pre-twisted tapered FG beam for various geometric and material parameters.

An experimental investigation of helicopter rotor blade was done in paper [30], where vibratory testing was done to test the material properties of composite helicopter blades. In their another paper [31] the author has done fatigue testing of helicopter rotor blade for composite laminated material. Static and dynamic experimental tests were performed by [32] for the rotor tail blade made up of composite laminated materials. The paper [33] discuss about the design of rotor blade of helicopter to satisfy the cross-sectional properties of composite material.

Other structural models where rotating effect is considered for static analysis is disc where authors like [34] has studied stresses and deformation of rotating FG disc for various boundary condition using finite element method. [35] has reported limit elastic speed analysis of rotating FG beam based on von mises criteria. [36] has also done analysis radial, tangential stress and strain for FG rotating disc. [37] and [38] has derived equation of motion for axial, flap wise and chordwise motion using Hamilton's principle and has analysed natural frequencies and time response for isotropic and FGM beam. [39] has studied vibrational behaviour and stress of perforated rotating beam using finite element analy–sis. The study shows the effect of perforated configu–ration and rotating speed on stress distribution and vib–ration response of the model. [40] has presented static response of porous rotating thick truncated cone for functionally graded material.

The present work lays the foundation of the mathe–matical formulation of rotating functionally graded beam using the B-spline collocation method and dis–cusses the static behaviour of such structures under the effect of different parameters. The effect of rotational speed on the deflection and stress distribution on the FG beam for various values of power index has been investigated for two different slenderness ratios. Based on the literature review, it is observed that there is hardly any literature present that directly deals with static analysis of functionally graded rotating beam. The structure of the paper is as follows: The subsequent section, i.e., section 2 presents the formulation of rotating beam using principle of virtual displacement where the property of materials used is varied in vertical direction. This section also introduces to the numerical method used to solve the governing equation i.e., B-spline collocation method. Verification of proposed numerical method is done by validating the preliminary results with those obtained using ANSYS and is reported in section 3. Section 4 reports and discusses the obtained results. Section 5 concludes and summarises the work reported in this article.

2. METHODOLOGY

A functionally graded cantilever beam of length $\boldsymbol{L}$, width $\boldsymbol{b}$, height $\boldsymbol{h}$ rotating at $\boldsymbol{\Omega}$ rad/sec is considered. The beam is fixed to a hub of radius, $\boldsymbol{r}$ and the hub is free to rotate about the vertical axis, as shown in figure 1. Material grading of the beam is assumed to vary in the transverse direction across the height of the beam according to the power law (1). The FG beam is made of metal on the top surface and ceramic on the bottom surface. The effective properties generalized as $\boldsymbol{P}$, i.e., young's modulus ($\boldsymbol{E}$), density($\boldsymbol{\rho}$), Shear modulus($\boldsymbol{G}$) and Poisson's ratio ($\boldsymbol{\mu}$) of the functionally graded beam, are evaluated using the power law function as follows:

$$\begin{aligned} E(z) &= (E_T - E_B)\left(\frac{z}{h}+\frac{1}{2}\right)^{\lambda} + E_B \\ \rho(z) &= (\rho_T - \rho_B)\left(\frac{z}{h}+\frac{1}{2}\right)^{\lambda} + \rho_B \\ G(z) &= \frac{k_s E(z)}{2(1+\mu(z))} \end{aligned} \tag{1}$$

where k_s is the shear correction factor [20], λ is the power index, T and B denote the top and bottom surfaces of the beam, (where the top and bottom surface comprises of metal and ceramic with young's modulus

as E_T, E_B respectively). Figure 2 shows the variation of the Young's Modulus along the height of beam.

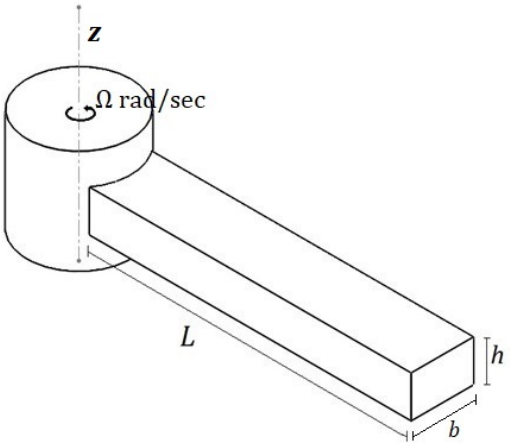

Figure 1. Rotating functionally graded cantilever beam.

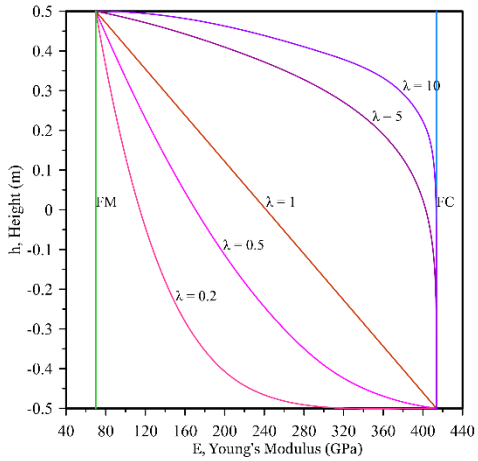

Figure 2. Variation of the Young's modulus along the height of the beam at different power index

The governing equations are derived using the principal of virtual work in the framework of Timoshenko beam theory to incorporate the effect of shear deformation. Displacement variables (u, v, w, and θ) are considered in the x, y, z-direction, and rotation of the cross section, respectively. The displacement field is taken as:

$$\begin{aligned} u(x,z) &= u_0(x) + z\theta \\ v(x,z) &= 0 \\ w(x,z) &= w(x) \end{aligned} \tag{2}$$

Here, u_0 and θ denotes axial displacement and rotation of the midplane. Therefore, normal strain ε_{xx} and shear deformation γ_{xz} for moderate deformation is given by:

$$\begin{aligned} \varepsilon_{xx} &= \left(\frac{\partial u_0}{\partial x} + \frac{1}{2}\left(\frac{\partial w}{\partial x}\right)^2\right) + \left(z\frac{\partial \theta}{\partial x}\right) \\ \gamma_{xz} &= \left(\frac{\partial w}{\partial x} + \theta\right) \end{aligned} \tag{3}$$

Using the principle of virtual work displacement, one can state that work done by the actual force is zero if and only if the body is in equilibrium. Therefore, the sum of the virtual work done by the internal and external forces is equal to zero.

$$\delta U_0 + \delta U_P + \delta U_R = 0 \tag{4}$$

δU_0, is the strain energy and is given by:

$$\delta U_0 = \int_0^L \int_A \left(\sigma_{xx}\delta\varepsilon_{xx} + \tau_{xz}\delta\gamma_{xz}\right) dA dx \tag{5}$$

$$\begin{aligned} \delta U_0 = \int_0^L \Bigg(N_{xx}\delta\left(\frac{\partial u_0}{\partial x} + \frac{1}{2}\left(\frac{\partial w}{\partial x}\right)^2\right) + \\ M_{xx}\left(\frac{\partial \theta}{\partial x}\right) + Q\delta\left(\frac{\partial w}{\partial x} + \theta\right)\Bigg) dx \end{aligned} \tag{6}$$

Here,

$$\begin{aligned} N_{xx} &= b\int_{-h/2}^{h/2} \sigma_{xx} dz; M_{xx} = b\int_{-h/2}^{h/2} z\sigma_{xx} dz \\ Q &= b\int_{-h/2}^{h/2} \tau_{xz} dz \end{aligned} \tag{7}$$

δU_R, is the external work done by centrifugal force on the beam.

$$\delta U_R = \frac{1}{2}\int_0^L N_R \left(\frac{\partial w}{\partial x}\right)^2 dx \tag{8}$$

$$\delta U_R = -\int_0^L \frac{\partial}{\partial x}\left(N_R \frac{\partial w}{\partial x}\right)\delta w \tag{9}$$

Centrifugal force N_R is given by.

$$\begin{aligned} N_R &= \int_A \int_x^L \rho\Omega^2 (R + x) dA dx \\ N_R &= \rho A\Omega^2 \left(R(L - x) + \frac{L^2 - x^2}{2}\right) \end{aligned} \tag{10}$$

δU_P, denotes the work done by uniformly distributed load 'q'.

$$\delta U_P = b\int_0^L q(x).w(x).dx \tag{11}$$

In the absence of applied axial force N_{xx}, substituting (6), (9), (11) in (4), the governing equation for rotating beam is given by.

$$\begin{aligned} \hat{E}_2 \frac{\partial^2 \theta}{\partial x^2} - G_0\left(\frac{\partial w}{\partial x} + \theta\right) = 0 \\ \frac{\partial}{\partial x}\left(G_0\left(\frac{\partial w}{\partial x} + \theta\right)\right) - \frac{\partial}{\partial x}\left(N_R \frac{\partial w}{\partial x}\right) + q = 0 \end{aligned} \tag{12}$$

Here

$$\begin{aligned} \hat{E}_2 &= E_2 - \frac{E_1^2}{E_0} \\ [E_0, E_1, E_2] &= \int_A E(x)(1, z, z^2) dA \end{aligned} \tag{13}$$

To simplify the calculation, (12) is converted into a single equation with a single unknown. Therefore, from [20]:

$$\begin{aligned} w &= F - \frac{\hat{E}_2}{G_0}\frac{\partial^2 F}{\partial x^2} \\ \theta &= -\frac{\partial F}{\partial x} \end{aligned} \tag{14}$$

where F is a new auxiliary function of length dimension. On substituting the above equation for *'w'* and *'θ'*, a single fourth order equation is obtained.

$$\hat{E}_2\left(1-\frac{N_R}{G_0}\right)\left(\frac{\partial^4 F}{\partial x^4}\right)+N_R\frac{\partial^2 F}{\partial x^2}+\frac{\partial N_R}{\partial x}\frac{\partial F}{\partial x}=q \tag{15}$$

In the absence of axial force, bending moment and shear force in the beam is given by:

$$M_{xx}=-\hat{E}_2\frac{\partial^2 F}{\partial x^2}, \quad Q=-\hat{E}_2\frac{\partial^3 F}{\partial x^3} \tag{16}$$

The authors, in their paper [20], have formulated the governing equations for a non-rotating beam and simplified them to a single equation whose solution is approached using direct integration method. However, in the present case it is difficult to obtain solutions using direct techniques available for non-linear cases. Hence the solutions to the governing equation for rotating FG beam is approached using numerical techniques. On solving (15) by using an appropriate numerical method, the auxiliary function 'F' can be determined which can be used to find other depended variables. In the present study solution of (15) is obtained using the collocation technique with b-spline basis as approximating function.

The B-spline collocation method provides a closed-form, piecewise continuous solution where the differential equation is satisfied at a finite number of points called collocation points. The parametric coordinate *'t'* is defined in terms of order of the resulting polynomial, also known as the knot vector. It is assumed that the knot vector is of open type given by:

$$T=[t_0,t_1,t_2,.....,t_{n+k+1}] \tag{17}$$

where, $n+1$ are the number of control points and *'k'* is the order of the polynomial spline. Once the knot vector is selected, B-spline basis function $N_{i,k}(t)$ is defined by a recursive relationship that is known as the Cox-de Boor recursion formula.

$$N_{i,1}(t)=\begin{cases}1.x_i\le t\le x_{i+1}\\ 0.otherwise\end{cases}$$
$$N_{i,k}(t)=\frac{(t-x_i)N_{i,k-1}(t)}{x_{i+k-1}-x_i}+\frac{(x_{i+k}-t)N_{i+1,k-1}(t)}{x_{i+k}-x_{i+1}} \tag{18}$$

The resulting B-spline curve is defined using the $(n+1)$ control points $B_0, B_1, B_2.... B_n$ and the basis function as:

$$F(t)=\sum_{i=1}^{n+1}B_i N_{i,k}(t), \quad where \quad t_{\min}\le t\le t_{max}, 2\le k\le n+1 \tag{19}$$

The above function 'F' is substituted in the governing equation as approximating polynomial such that it satisfies the given boundary conditions. As the number of unknowns in approximating polynomial exceeds the number of boundary conditions, hence we need to force the solutions at discrete points called ***collocation*** points. In this study, the collocation points or abscissa control points are selected using the Grevillea abscissa approach. The position vector of the control point 'B_i' used to define the B-spline curve with the parametric coordinate 't' is calculated as follows:

$$x_i=\frac{1}{n}(t_i+t_{i+1}+...+t_{i+n-1}) \tag{20}$$

In the current analysis, a polynomial of degree 4 or above will be suitable to solve (15). A sixth-order polynomial (fifth degree) has been selected using open-uniform knot vector with no intermediate points to act as an approximating polynomial. Considering the case of material and geometric nonlinearity related to problem and to investigate wider levels of research, a higher order of b-spline functions is taken. A MATLAB code is developed indigenously to numerically investigate the problem of rotating FG beams.

3. VERIFICATION OF METHOD WITH ANSYS

To verify the correctness and accuracy of the present method, the results obtained by the B-spline collocation method are compared with the results obtained through commercial finite element package of ANSYS. A rotating cantilever beam of uniform cross-section with length of beam = 0.5 m and height = 0.125 is considered. The materials used for the FG beam are of ceramic metal composition, which specifically have the following properties: Metal part is aluminium with young's modulus= 70GPa, density = 2700Kg/m^3, poison's ratio =0.3 while the ceramic material is silicon carbide with young's modulus = 413.68GPa, density = 3100kg/m^3 and poison's ratio =0.3. The beam rotates at a uniform speed of Ω=100 rad/sec.

The response of rotating beam is investigated using the MATLAB code developed as per the mathematical formulation discussed in previous section and is verified using the ANSYS software. Comparison between the obtained result for deflection and normal stresses in Figure 3 and Table 1 shows that a good agreement exists between results obtained using MATLAB and ANSYS.

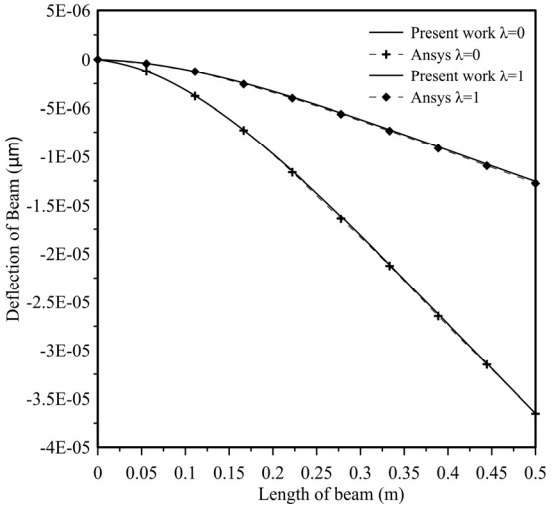

Figure 3. Deflection for isotropic and functionally graded rotating beam at Ω=100 rad/sec

Table 1: Normal Stress for isotropic and functionally graded rotating beam

Normalized Stress	Present Work	ANSYS	Error %
$\lambda = 0$	12.0238	11.8795	1.2%
$\lambda = 1$	18.8474	17.9860	4.6%

4. RESULTS AND DISCUSSION

In the present study, the static deflection characteristic and stress distribution in a rotating functionally graded beam have been investigated. The rotating beam is assumed to be composed of metal and ceramic; the mate–rial properties smoothly vary according to the power law across the height of the beam; properties of material have been listed in Table 2. Two cases have been taken with slenderness ratio L/h=10 and L/h=20 of constant cross-section i.e., height and width =0.125 m. The proposed computational model is used to inves–tigate the effect of centrifugal force on stress distri–bution as well as deflection throughout the beam under self-body weight.

Table 2: Material Properties of a functionally graded rotating cantilever beam.

Material Property	Aluminium (Metal)	Silicon carbide (Ceramic)
Young's Modulus, (G Pa)	70	413.169
Density, (Kg/m^3)	2707	3100
Poisson's ratio	0.3	0.3

4.1 Effect of Rotation

The effect of rotation on functionally graded beams at different speeds and at specific power gradient has been investigated. The centrifugal force generated due to rotation shows different behavior for the slenderness ratio L/h=10 and L/h=20 on static deflection and stresses. Transverse deflection for different rotating speeds at a specific power gradient are shown in figure 4 and 5 at slenderness-ratio (L/h) 10, 20 respectively. From the figure it can be depicted that, under non-rotating conditions, i.e., Ω=0 rad/sec, the beam deflects under self-weight and as soon as rotation is given, this deflection starts to increase. The deflection increases further as the rotational speed increases. In the case of L/h = 10 (Figure 4) typical behavior in deflection is observed where higher speeds give higher deflections.

The gap amongst deflection at different speeds conti–nues to decrease with increasing power gradient, which is the lowest for ceramics and at λ=5 whereas for metal the gap is the highest. Stiffness of the structure depends on the two factors, firstly on stiffness of the material and secondly on the geometry of the structure. Higher value of power index increases the stiffness whereas higher value of slenderness ratio reduces the stiffness. For the slenderness ratio, L/h = 20, Figure 5 shows an incon–sistent behavior, where the beam deflects downwards till Ω=100 rad/sec and thereafter the beam deflects upward. This is due to the increase in length of the beam, which in turn decreases the flexural rigidity. This flexural rigidity increases with increase in the material gradient as it can be seen from the figure that the beam axis is moving toward the neutral axis with increasing power gradient.

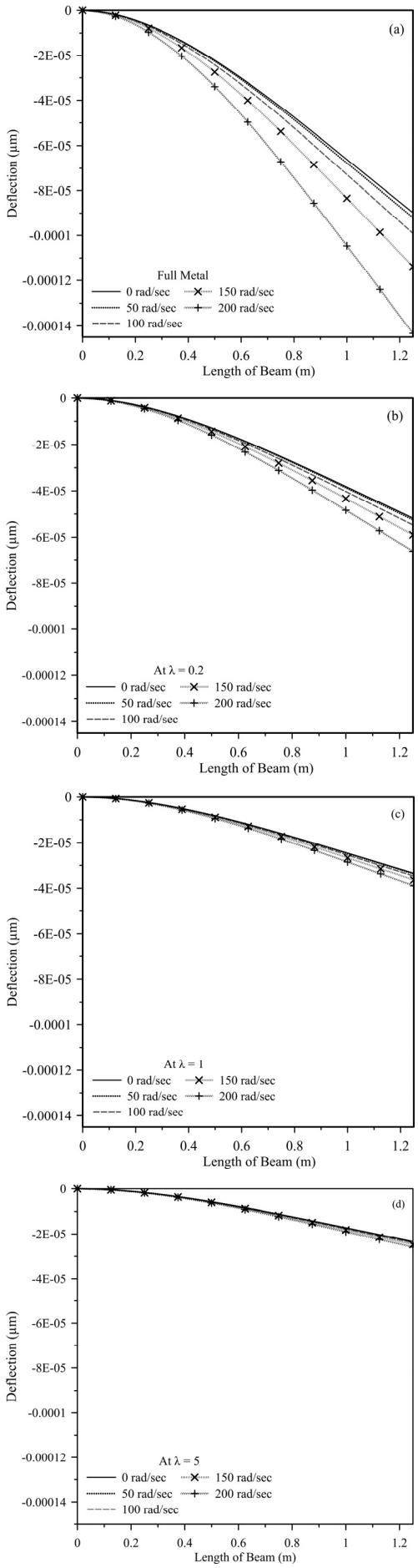

Figure 4. Deflection at different rotational speed for λ= full metal(a), 0.2(b), 1(c), 5(d) for the L/h=10

The comparison of the induced normal stresses with the slenderness ratio (L/h) 10, 20 is presented in Figures 6 and 7, showing the normal stresses for different speeds for specific material gradation. For L/h = 10, the graph shows smooth variation of normal stresses along the height of the beam for functionally graded material, where there is an increase in the normal stress with increase in the rotational speed at all the value of power gradient. However, the effect of an increase in centrifugal force with rotational speed is minimal in the case of L/h=10.

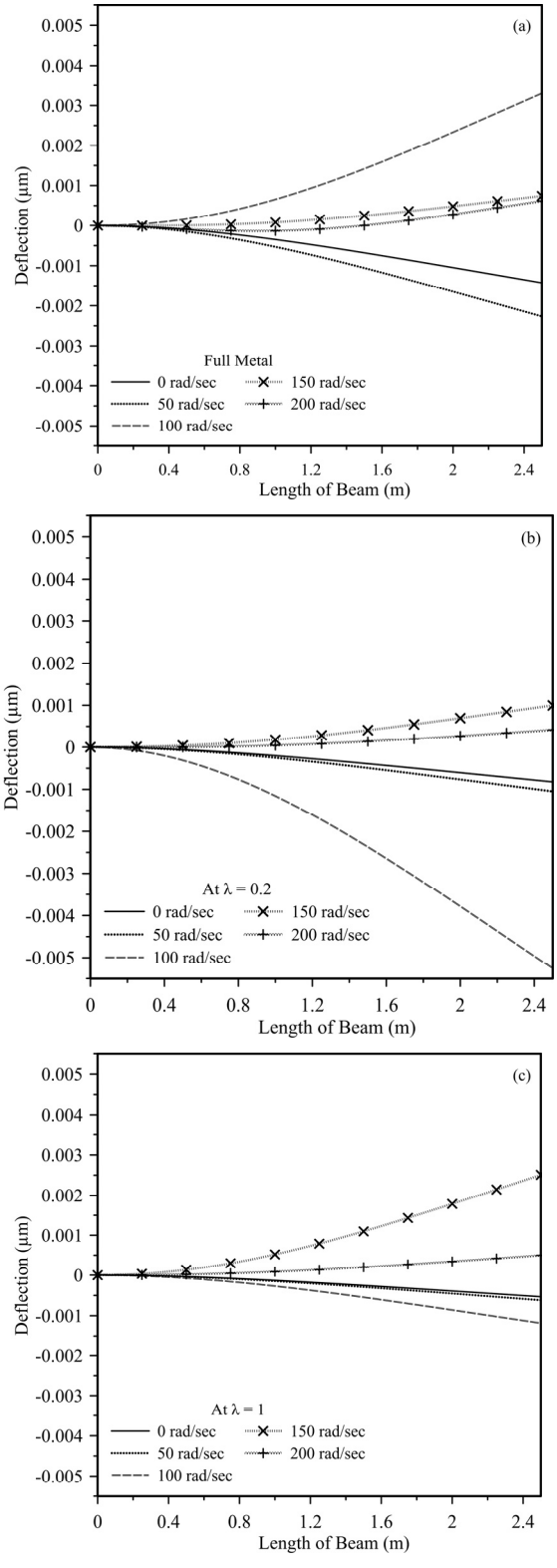

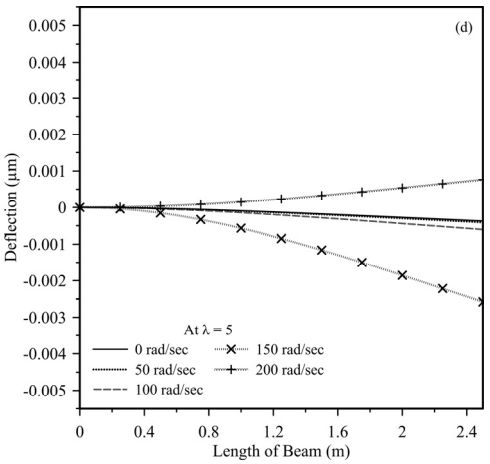

Figure 5. Deflection at different rotational speed for λ= full metal(a), 0.2(b), 1(c), 5(d) for L/h=20

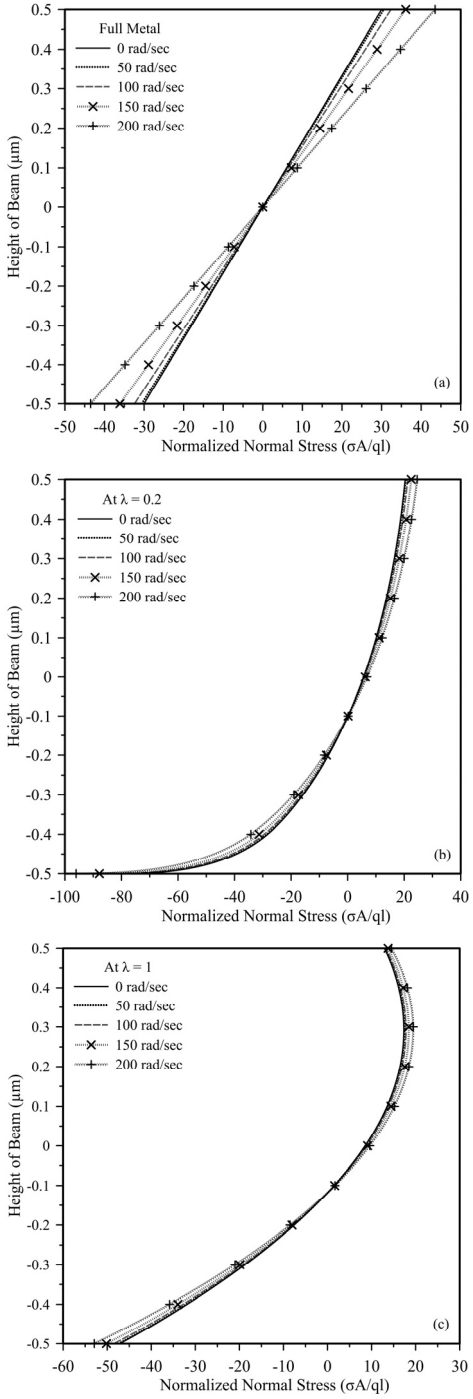

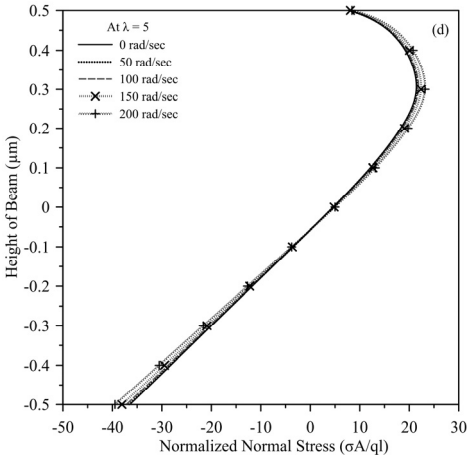

Figure 6. Normal stress at different rotational speed for λ= full metal(a), 0.2(b), 1(c), 5(d) for L/h=10

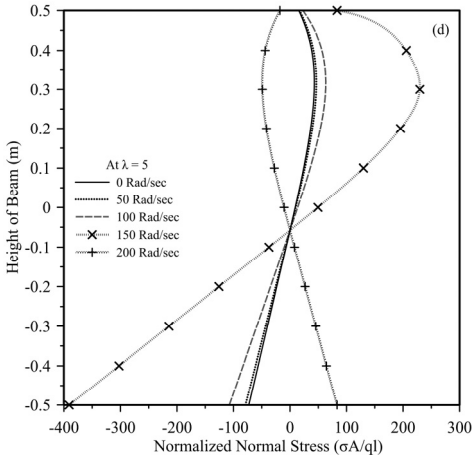

Figure 7. Normal stress at different rotational speed for λ= full metal(a), 0.2(b), 1(c), 5(d) for L/h=20

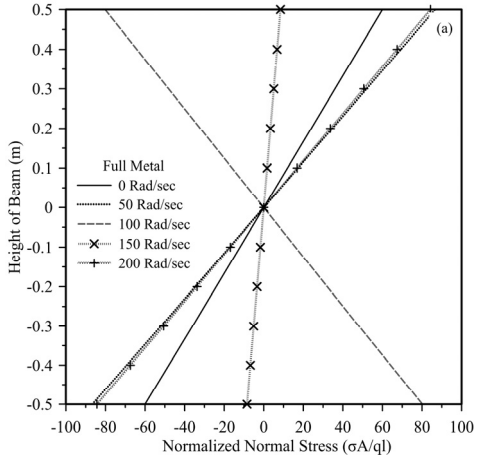

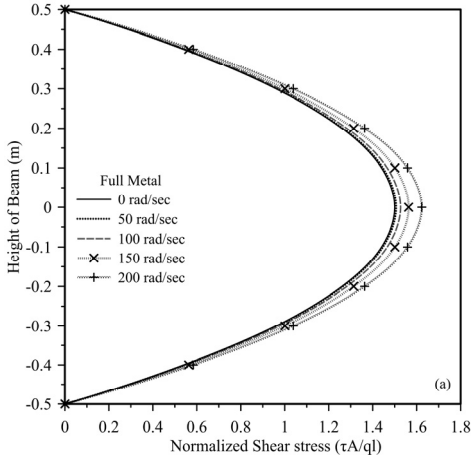

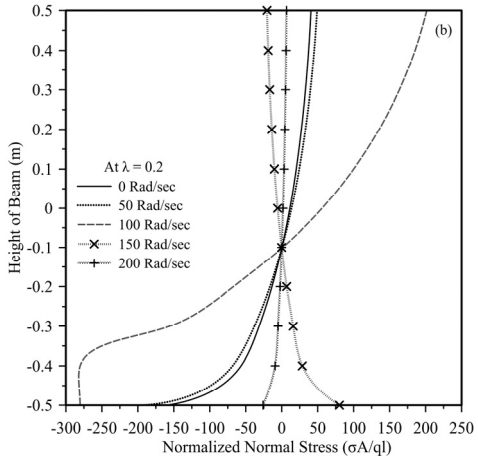

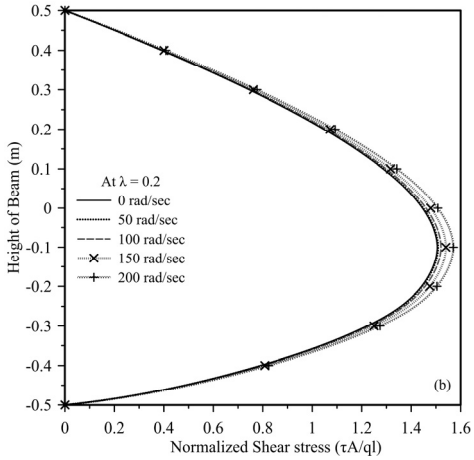

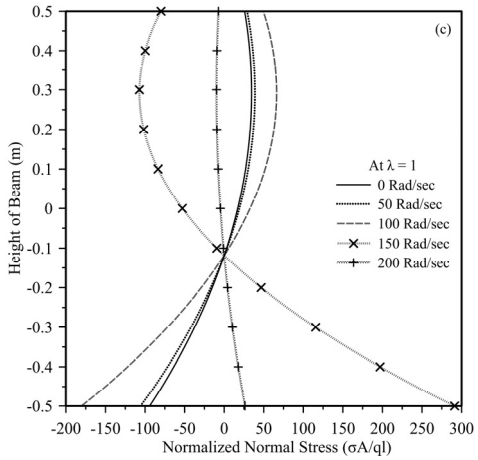

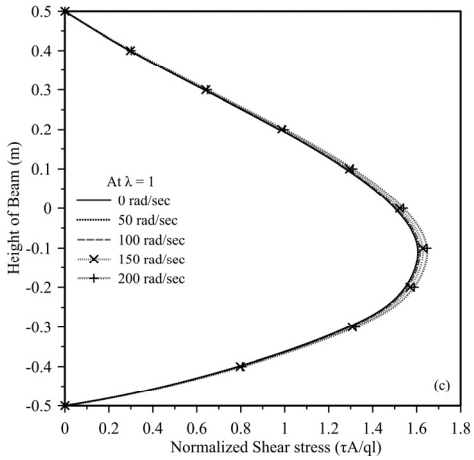

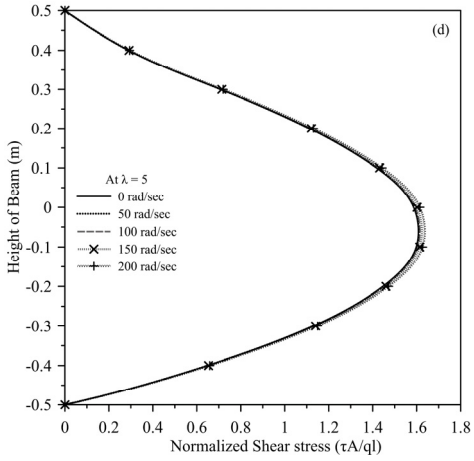

Figure 8. Shear stress at different rotational speed for λ= full metal(a), 0.2(b), 1(c), 5(d) for L/h=10

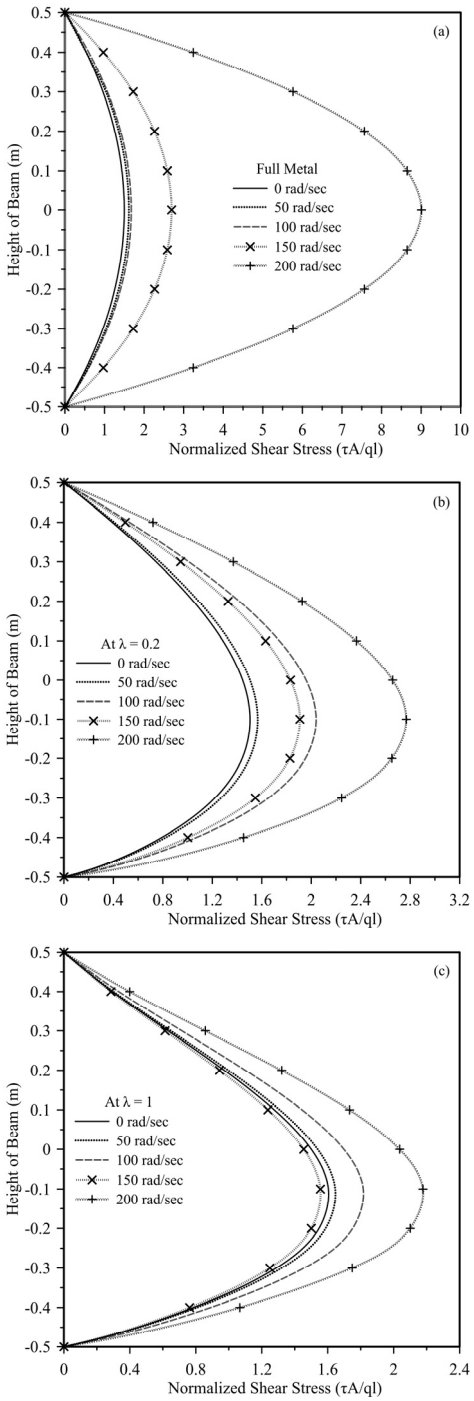

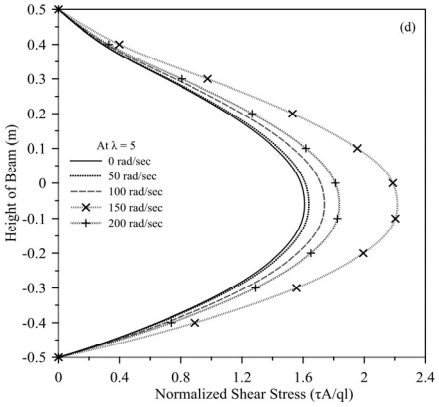

Figure 9. Shear stress at different rotational speed for λ= full metal(a), 0.2(b), 1(c), full ceramic(d) for L/h=20

For L/h=20, a typical variation of normal stresses is observed due to decrease in flexural rigidity. The normal stresses for Ω = 0, 50 rad/sec shows the tensile stress on the upper surface and the compressive stress on the lower surface. At Ω = 100 rad/sec a sudden change in the direc–tion of normal stress is observed due to fluctuation of beam in upward direction. On further increase in rotational speed, the normal stress is reported to increase.

Similarly, for shear stresses, the effect of rotation is least for of L/h = 10 as shown in Figure 8. The maxi–mum shear stress increases with increase in the rota–tional speed, and this increase in the maximum stresses is reduced with increase in power gradient. For a slenderness ratio of L/h = 20, Figure 9 shows that shear stress increases with increase in rotational speed. How–ever, the fluctuation in the shear stress is observed at the rotational speed of Ω = 100, 200 rad/sec. For metal, the maximum shear stress is quite high for Ω = 200 rad/sec. Hence the alteration in shear stress is relatively high in case of L/h =20 and least in case of L/h = 10.

4.2 Effect of Power Gradation

Figures 10 and 11 present the influence of the power gradient on the deflection and stresses of the rotating beam as the centrifugal stiffness increases with the increase in the rotation speed. Figure 10 shows that in the slenderness ratio L/h = 10, the increasing material gradient increases the stiffness of the material; as a result, there is a decrease in the deflection. Maximum deflection is for full metal at non-rotating and rotating condition, while least for ceramic and λ = 5. For a non-rotating beam under self-load, the beam deflection keeps decreasing with increasing power gradient.

As soon as the beam starts rotating due to centrifugal force, the deflection in the beam increases. At 100 rad / sec, the metal with the lowest value for flexural rigidity is overshadowed by centrifugal stiffness; with further inc–rease in rotational speed, the beam with a lower value of the material gradient, i.e., λ =0.2 shows a higher deflec–tion. At higher speeds, the stiffness due to the centrifugal force overcomes the flexural stiffness due to the material gradient and the beam deflects in the upward direction. For pure metal due to the least flexible stiffness, the material deflects first in the upward direc–tion followed by the beam at λ=0.2, 0.5, 1, 5 and ceramic with increasing rotational speed.

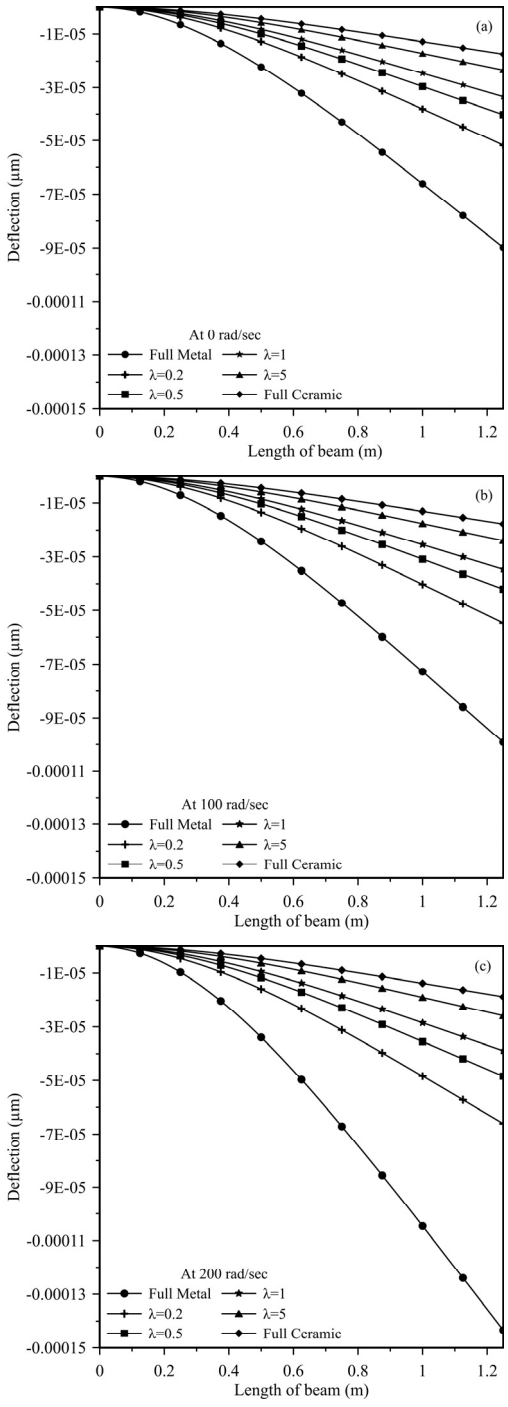

Figure 10. Deflection at different power index for the Ω= 0(a), 100(c),200(d) for slenderness ratio L/h=10

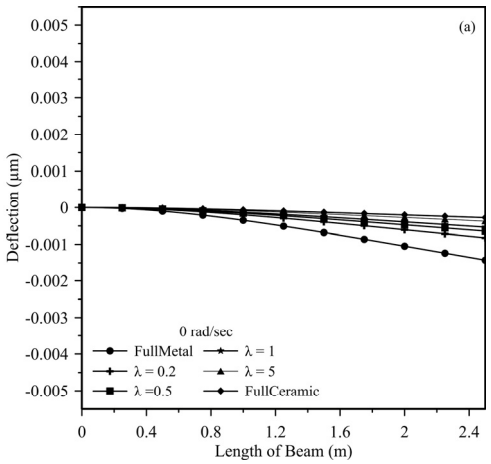

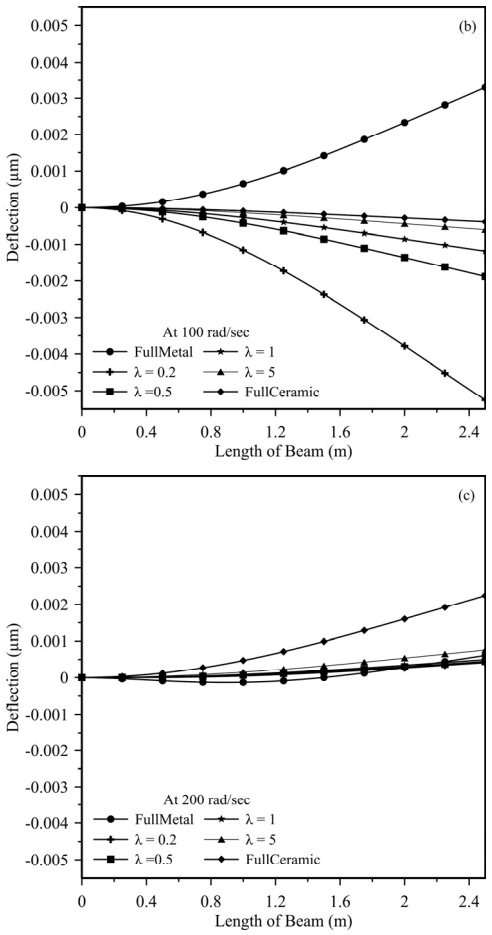

Figure 11. Deflection at different power index for Ω= 0(a), 100(c), 200(d) for slenderness ratio L/h=20

Figure 12 shows a change in normal stress with rotational speed where the stress varies linearly for isot–ropic material and non-linearly for functionally graded material. For rotating as well as non-rotating beam the tensile stress on top surface and compressive stress on bottom surface decreases with increase in power gradi–ent for L/h =10. Although for the slenderness ratio of L/h = 20 (Figure 13), there is a decrease in normal stress, however, the distribution fluctuates with an increase in the power gradient at higher rotational speed. At Ω =200 rad/sec, minimum normal stresses are ob–tained at λ =0.2 while for lower speed minimum normal stresses is obtained at λ = 5.0.

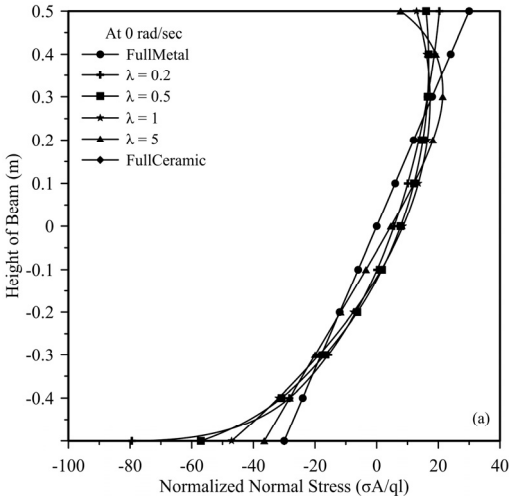

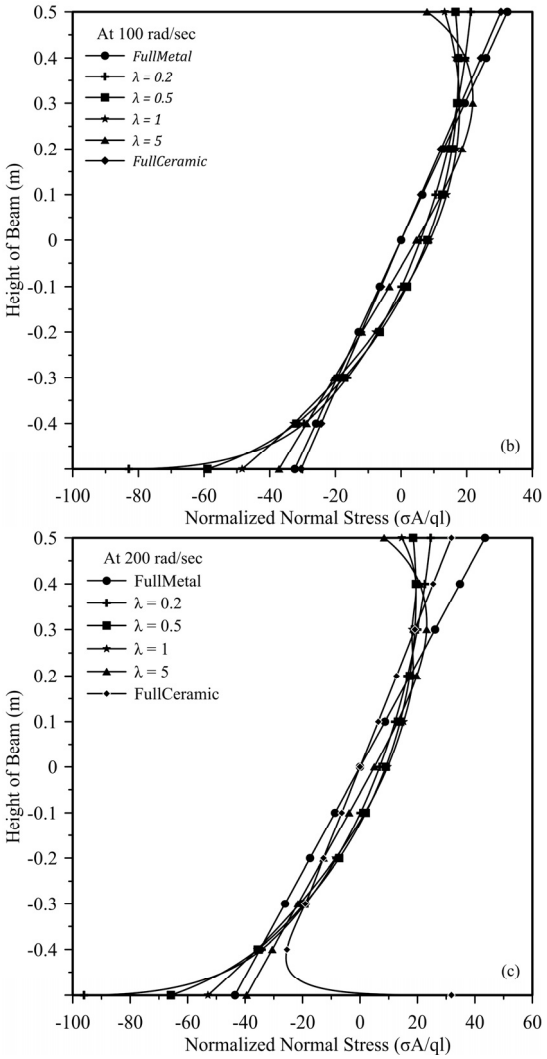

Figure 12. Normal stress at different value of power index for Ω= 0(a), 100(c),200(d)for slenderness ratio L/h=10

Figure 14 and 15 shows variation of shear stress across the height of the beam. In both cases, of slenderness ratio L/h =10 and 20, the centroidal axis of the beam and the neutral axis for complete metal and complete ceramic beams coincide, while for the power gradient λ =0.2, 0.5,1 the neutral axis moves downward away from the centroidal axis of the beam.

After λ = 5, the neutral axis moves back towards the centroidal axis. However, there is an increase in shear stress with increase in power gradient for non-rotating beam at λ =full metal, 0.2, 0.5, 1, 5. On further increase in power gradient, the maximum value of shear stress decreases. In the case of a rotating beam, the minimum value of maximum shear stress is obtained at power gradient λ =0.2. Maximum value of shear stresses for L/h=20 is higher as compared to L/h =10. An enormous increase in the shear stress is observed for full metal case at the rotational speed of 200 rad/sec, while for other power index, not much increase in the value of shear stress is reported.

4.3 Effect of rotation along the length of the beam

Normal stresses along the beam length for slenderness ratio of L/h =10, 20 have been compared in Figure 16 for λ= 0.2, 1, 5 at 200 rad/sec. In both cases the normal stress at the free end gives linear vertical curve whose value is zero across the height of the beam. As one moves towards the fixed end, the curvature of nonlinear curves increases along the length at L/4, L/2, 3L/4, L distance from fixed end of the beam.

The beam deflection for L/h =20 in figure 16 (c), (d) is in opposite direction to that of L/h=10 in figure 16 (a), (b) at 200 rad / sec, therefore, the direction of the deflection curve for normal stresses is also in the opposite direction. Similar is the case for shear stresses shown in Figure 17, where due to fluctuation of beam in upward direction at 200 rad/sec, there is a shift in the shear stress distribution for slenderness ratio L/h= 20 as compared to the beam with L/h=1.

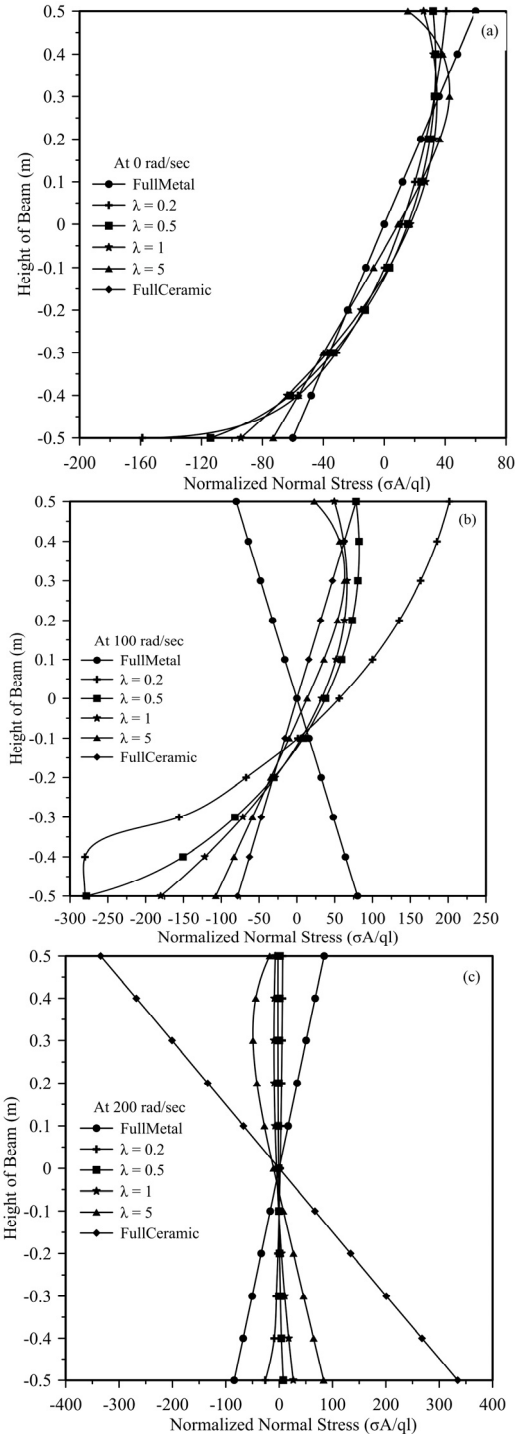

Figure 13. Normal stress with respect of rotation for Ω= 0(a), 100(c), 200(d) for slenderness ratio L/h=20

5. CONCLUSION

The B-spline collocation method is a numerical techni–que suitable for use with standard geometries, like rec–tangles, that provides piecewise-continuous, closed-form solution. A MATLAB code was developed to solve the mathematical model of a rotating functionally graded beam. The solution obtained is verified using the ANSYS software. In this work, the static behaviour of a trans–versally functionally graded rotating beam is presented.

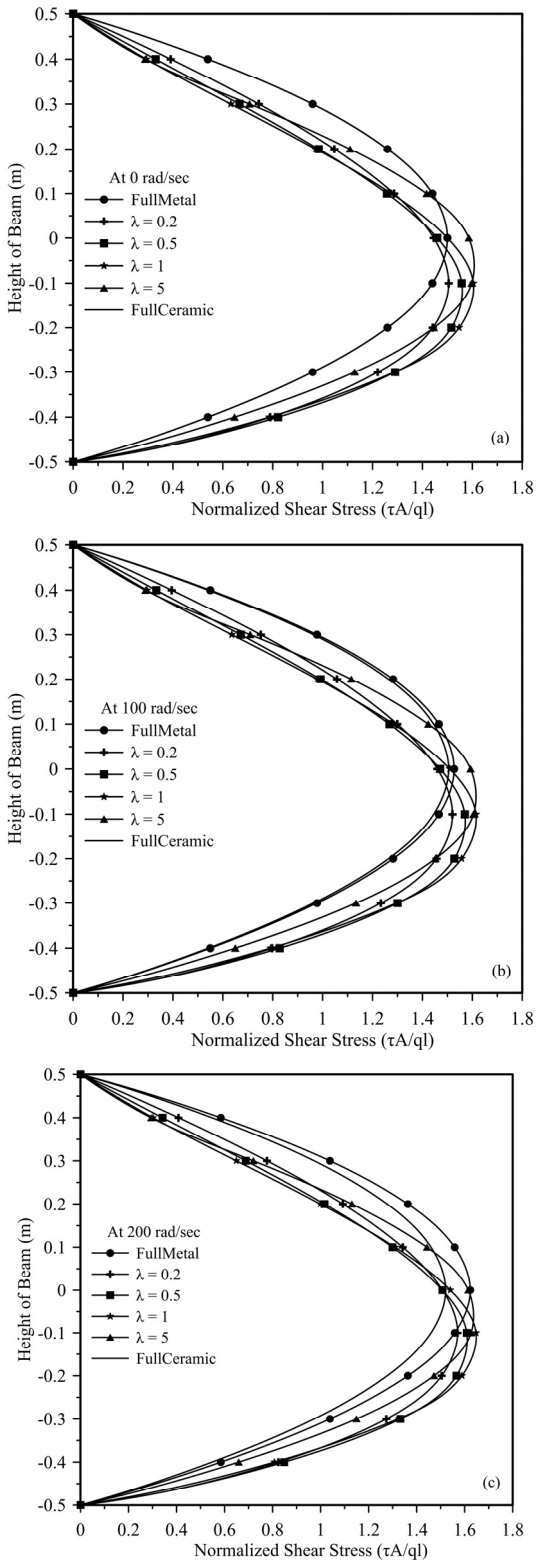

Figure 14. Shear stress with respect of rotation for Ω= 0(a), 100(c), 200(d) for slenderness ratio L/h=10

This study appears to be the first to analyse the effect of functional grading on deflection and the stresses developed when the beam is under the influence of centrifugal force such as those found in the appli–cations of rotor blades and slender rotating structures. The results also highlights the crucial part played by slenderness ratio in stability of the rotating beam and effect of functional grading on slenderness ratio.

Effect of both power index and rotational speed on the material of beam is observed. An increase in rota–tional speed increases deflection and stresses, whereas an increase in power index decreases the value of deflection and stresses.

1. The deflection reduces with increase in power index. However, though least value of deflection is observed in ceramics, but the normal stresses are reported to be highest.
2. The slenderness ratio plays an important role in the behaviour of the beam, where the beam with a higher slenderness ratio shows instability with an increase in rotational speed due to a decrease in flexural stiffness.
3. Along the length of the beam both normal and shear stress goes on reducing from fixed end towards the free end where the stresses are zero.
4. At neutral axis, minimum value of normal stress and maximum value of shear stress is analysed at power index λ=0.2 at all the rotational speed. Therefore, λ=0.2 gives best response for normal and shear stress.

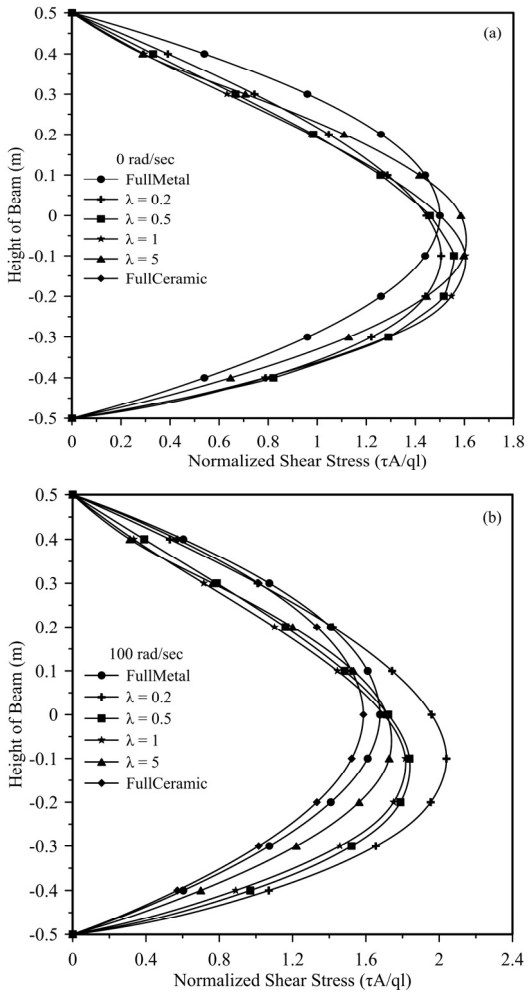

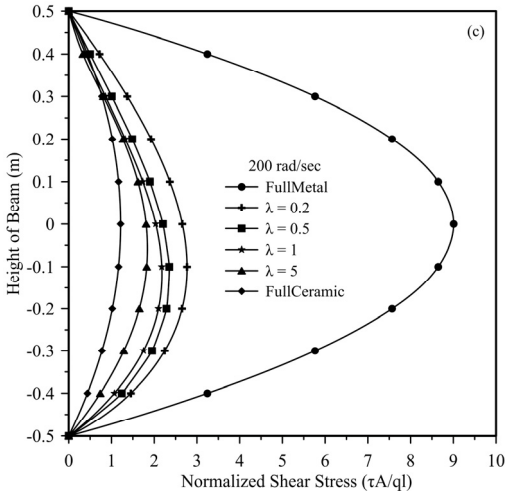

Figure 15. Shear stress with respect of rotation for Ω= 0(a), 100(b), 200(c) for slenderness ratio L/h=20

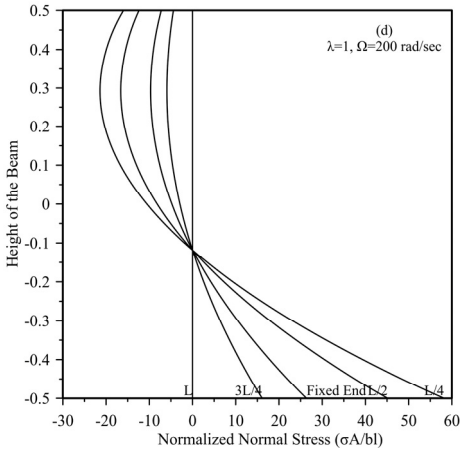

Figure 16: Normal stress along the length of the beam for L/h=10 (a)(b), 20(c)(d) at length L, 3L/4, L/2, fixed end

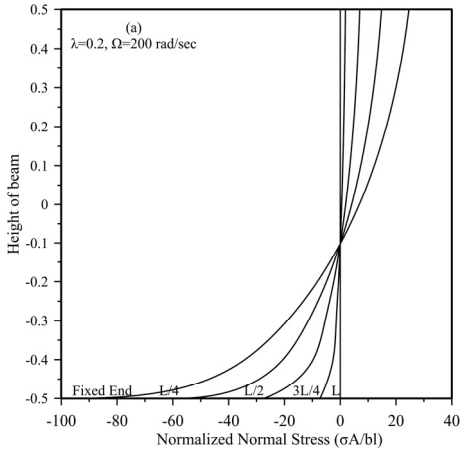

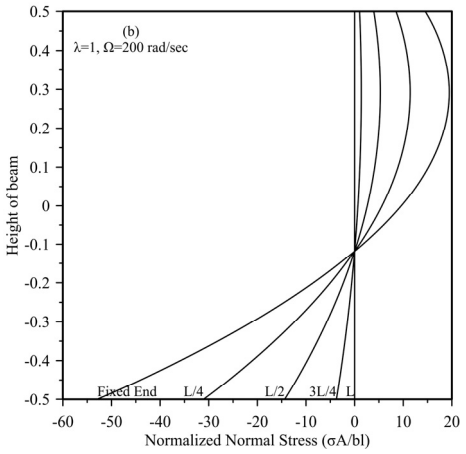

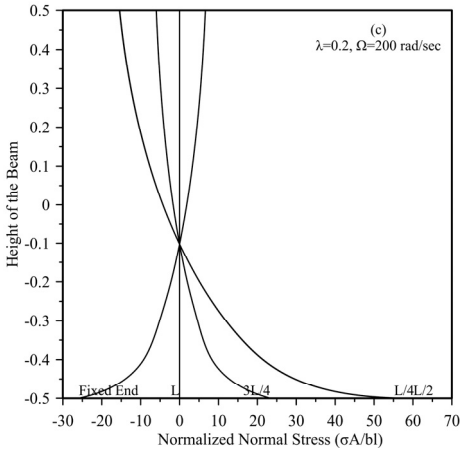

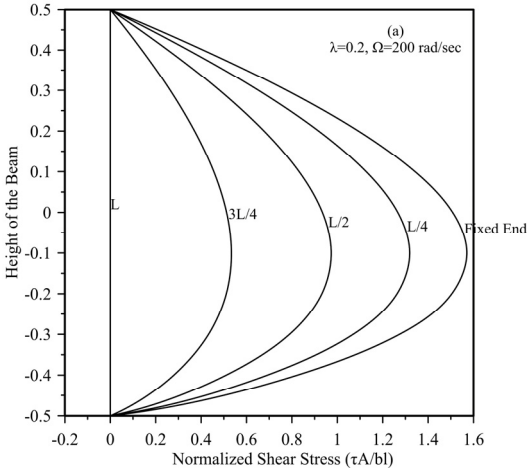

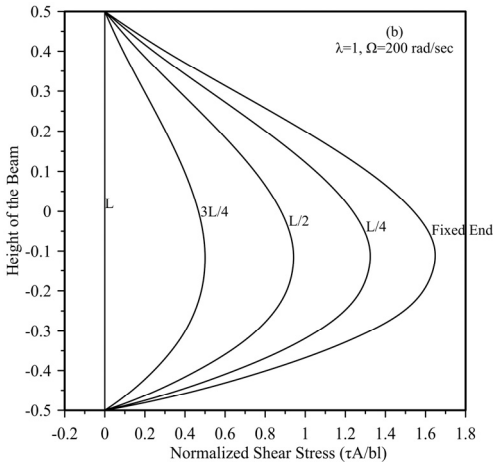

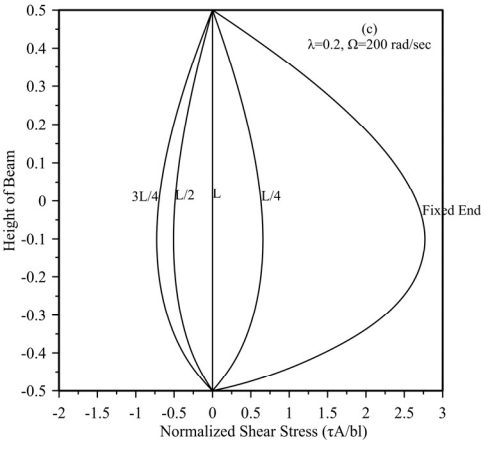

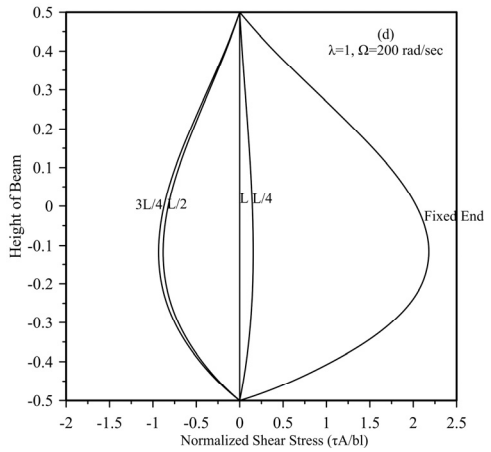

Figure 17: Shear stress along the length of the beam for L/h=10 (a), (b), and 20 (c), (d) at length L, 3L/4, L/2, 0

ACKNOWLEDGEMENT

The authors gratefully acknowledge National institute of technology, Raipur for their support and providing plat–form for this research.

REFERENCES

[1] K. Ahmad, Y. Baig, H. Rahman, and H. J. Hasham, 'Progressive failure analysis of helicopter rotor blade under aeroelastic loading', *Aviation*, vol. 24, no. 1, pp. 33–41, Mar. 2020, doi: 10.3846 /aviation.2020.12184.

[2] P. M. Pawar, R. Ganguli, 'On the effect of progres–sive damage on composite helicopter rotor system behavior', *Compos Struct*, vol. 78, no. 3, pp. 410–423, May 2007, doi: 10.1016/j.compstruct.2005.11.043.

[3] M. Amura, L. Aiello, M. Colavita, F. De Paolis, and M. Bernabei, 'Failure of a Helicopter Main Rotor Blade', *Procedia Materials Science*, vol. 3, pp. 726–731, 2014, doi: 10.1016/j.mspro.2014. 06.119.

[4] J. Babu Gunda, R. Ganguli, 'New rational inter-polation functions for finite element analysis of rotating beams', *Int J Mech Sci*, vol. 50, no. 3, pp. 578–588, Mar. 2008, doi: 10.1016/j.ijmecsci. 2007.07.014.

[5] D. Garinis, M. Dinulović, and B. Rašuo, 'Dynamic analysis of modified composite helicopter blade', *FME Transactions*, vol. 40, no. 2, pp. 63–68, 2012.

[6] A. Chakraborty, S. Gopalakrishnan, J. N. Reddy, 'A new beam finite element for the analysis of functionally graded materials', *Int J Mech Sci*, vol. 45, no. 3, pp. 519–539, Mar. 2003, doi: 10.1016-/S0020-7403(03)00058-4.

[7] H. Du, M. K. Lim, K. M. Liew,' A power series solution for vibration of rotating Timoshenko beam' *J Sound Vib*, vol. 175, no. 4, pp. 505-523, Mar. 1994.

[8] G. Oliveto, 'Dynamic Stiffness and Flexibility Fun-ctions for Axially Strained Timoshenko Beams', vol. 154, no. 1, pp. 1-23, Jan 1992.

[9] S. C. Lin, K. M. Hsiao, 'Vibration analysis of a rotating Timoshenko beam', *J Sound Vib*, vol. 240, no. 2, pp. 303–322, Feb. 2001, doi: 10.1006/jsvi. 2000.3234.

[10] C. L. Huang, W. Y. Lin, K. M. Hsiao, 'Free vibration analysis of rotating Euler beams at high angular velocity', *Comput Struct*, vol. 88, no. 17–18, pp. 991–1001, 2010, doi: 10.1016/j.compstruc. 2010.06.001.

[11] J. Chung, H. H. Yoo, 'Dynamic analysis of a rotating cantilever beam by using the finite element method', *J Sound Vib*, vol. 249, no. 1, pp. 147–164, Jan. 2002, doi: 10.1006/jsvi.2001.3856.

[12] M. T. Piovan, R. Sampaio, 'A study on the dynamics of rotating beams with functionally graded properties', *J Sound Vib*, vol. 327, no. 1–2, pp. 134–143, Oct. 2009, doi: 10.1016/j.jsv.2009.06.015.

[13] M. O. Kaya, 'Free vibration analysis of a rotating Timoshenko beam by differential transform met-hod', *Aircraft Engineering and Aerospace Techno-logy*, vol. 78, no. 3, pp. 194–203, 2006, doi: 10.1108/17488840610663657.

[14] F. Ebrahimi, S. Dashti, 'Free vibration analysis of a rotating non-uniform functionally graded beam', *Steel and Composite Structures*, vol. 19, no. 5, pp. 1279–1298, 2015, doi: 10.12989/scs.2015.19.5 .1279.

[15] J. R. Banerjee, 'Dynamic stiffness formulation and free vibration analysis of centrifugally stiffened Timoshenko beams', J Sound Vib, vol. 247, no. 1, pp. 97–115, Oct. 2001, doi: 10.1006/jsvi. 2001.3716.

[16] D. Chen, K. Feng, S. Zheng, 'Flapwise vibration analysis of rotating composite laminated Timo-shenko microbeams with geometric imperfection based on a re-modified couple stress theory and isogeometric analysis', European Journal of Mechanics, A/Solids, vol. 76, pp. 25–35, Jul. 2019, doi: 10.1016/j.euromechsol.2019.03.002.

[17] D. Mahapatra, 'A study of stress and deformation behaviour of functionally graded Timoshenko cantilever beam' Int J of advancement in manage-ment, technology, and engineering science', vol. 8, no. 3, pp. 1317–1321, Mar. 2018

[18] A. Bazoune, 'Effect of tapering on natural frequ-encies of rotating beams', IOS Press, 2007.

[19] G. Wang, N. M. Wereley, 'Free vibration analysis of rotating blades with uniform tapers', *AIAA Journal*, vol. 42, no. 12, pp. 2429–2437, 2004, doi: 10.2514/1.4302.

[20] X. F. Li, 'A unified approach for analysing static and dynamic behaviours of functionally graded Timoshenko and Euler-Bernoulli beams', J Sound Vib, vol. 318, no. 4–5, pp. 1210–1229, Dec. 2008, doi: 10.1016/j.jsv.2008.04.056.

[21] K. Sarkar and R. Ganguli, 'Rotating beams and non-rotating beams with shared eigenpair for pinned-free boundary condition', Meccanica, vol. 48, no. 7, pp. 1661–1676, Sep. 2013, doi: 10.1007/ s11012-013-9695-x.

[22] S. Rajasekaran, 'Free vibration of centrifugally stiffened axially functionally graded tapered

Timoshenko beams using differential transformation and quadrature methods', Appl Math Model, vol. 37, no. 6, pp. 4440–4463, Mar. 2013, doi: 10.1016/j.apm.2012.09.024.

[23] Y. Huang and X. F. Li, 'A new approach for free vibration of axially functionally graded beams with non-uniform cross-section', J Sound Vib, vol. 329, no. 11, pp. 2291–2303, May 2010, doi: 10.1016/j.jsv.2009.12.029.

[24] A. Sahu, N. Pradhan, and S. K. Sarangi, 'Static and Dynamic Analysis of Smart Functionally Graded Beams', *Proceedings of IConAMMA_2018*, 24 (2020) 1618–1625 www.materialstoday.com/ proceedings

[25] K. H. Almitani, M. A. Eltaher, A. A. Abdelrahman, and H. E. Abd-El-Mottaleb, 'Finite element-based stress and vibration analysis of axially functionally graded rotating beams', Structural Engineering and Mechanics, vol. 79, no. 1, pp. 23–33, Jul. 2021, doi: 10.12989/sem.2021.79.1.023.

[26] Y. Chen, X. Guo, D. Zhang, L. Li, 'Dynamic modelling and analysis of rotating FG beams for capturing steady bending deformation', Appl Math Model, vol. 88, pp. 498–517, Dec. 2020, doi: 10.1016/j.apm.2020.06.035.

[27] O. Thomas, A. Sénéchal, J. F. Deü, 'Hardening /softening behaviour and reduced order modelling of nonlinear vibrations of rotating cantilever beams', Nonlinear Dyn, vol. 86, no. 2, pp. 1293–1318, Oct. 2016, doi: 10.1007/s11071-016-2965-0.

[28] H. Lohar, A. Mitra, 'Nonlinear Free Vibration Analysis of Non-uniform Axially Graded Beam on Variable Elastic Foundation', FME Transactions, vol. 50, no. 4, pp. 643–654, 2022, doi: 10.5937/fme2204643L.

[29] Y. Oh, H. H. Yoo, 'Vibration analysis of rotating pre-twisted tapered blades made of functionally graded materials', Int J Mech Sci, vol. 119, pp. 68–79, Dec. 2016, doi: 10.1016/j.ijmecsci.2016.10.002.

[30] B. Rasuo, 'Experimental study of structural damping of composite helicopter blades with different cores', Plast. Rubber Compos., vol. 39, no. 1, pp. 1–5, 2010, doi: 10.1179/174328910X12608851832 092.

[31] B. Rasuo, 'Full-Scale Fatigue Testing of the Helicopter Blades from Composite Laminated Materials in the Development Process', J. Mech. Behav. Mater., vol. 19, no. 5, pp. 331–339, 2011, doi: 10.1515/jmbm.2009.19.5.331.

[32] B. Rasuo, 'Experimental Techniques for Evaluation of Fatigue Characteristics of Laminated Constructions from Composite Materials: Full-Scale Testing of the Helicopter Rotor Blades', Journal of Testing and Evaluation (JTE), Volume 39, Issue 2, 2011, ASTM International, USA, pp. 237-242. doi: 10.1520/JTE102768.

[33] S. L. Lemanski, P. M. Weaver, G. F. J. Hill, "Design of composite helicopter rotor blades to meet given cross-sectional properties," Aeronaut. J., vol. 109, no. 1100, pp. 471–475, 2005, doi: 10.1017/S0001924000000889.

[34] M. H. Jalali, B. Shahriari, 'Elastic Stress Analysis of Rotating Functionally Graded Annular Disk of Variable Thickness Using Finite Difference Method', Math Probl. Eng, vol. 2018, 2018, doi: 10.1155/2018/1871674.

[35] L. Sondhi, S. Sanyal, K. Saha, S. Bhowmick, 'Limit elastic speeds of functionally graded annular disks', FME Transactions, vol. 46, no. 4, pp. 603–611, 2018, doi: 10.5937/fmet1804603S.

[36] Manish Garg, 'Stress analysis of variable rotating FG disc', Int J pure and Appl. physics, vol. 13, no. 1, pp. 158-161, 2022

[37] H. Kim, H. Hee Yoo, J. Chung, 'Dynamic model for free vibration and response analysis of rotating beams', J Sound Vib., vol. 332, no. 22, pp. 5917–5928, Oct. 2013, doi: 10.1016/j.jsv.2013.06.004.

[38] Di. Zhou, J. Fang, H. Wang, and X. Zhang, 'Three-Dimensional Dynamics Analysis of Rotating Functionally Gradient Beams Based on Timoshenko Beam Theory', Int J Appl Mech, vol. 11, no. 4, May 2019, doi: 10.1142/S1758825119500406.

[39] M. A. Eltaher, H. E. Abdelmoteleb, A. A. Daikh, A. A. Abdelrahman, 'Vibrations and stress analysis of rotating perforated beams by using finite elements method', Steel and Composite Structures, vol. 41, no. 4, pp. 505–520, Nov. 2021, doi: 10.12989/scs.2021.41.4.505.

[40] M. Babaei, K. Asemi, 'Stress analysis of functionally graded saturated porous rotating thick truncated cone', Mechanics Based Design of Structures and Machines, vol. 50, no. 5, pp. 1537–1564, 2022, doi: 10.1080/15397734.2020.1753536.

NOMENCLATURE

L, b, h	Length, width, and thickness of the beam geometry respectively
L/h	Slenderness ratio.
Ω	Rotational speed
E, ρ	Young's modulus and density along the height of beam
E(z), ρ(z)	Young's modulus and density along the height of beam
G(z)	Shear modulus along the height of beam
G_0	Shear modulus
μ	Poisson's ratio
λ	Power index
u, v, w	Displacement variable in x, y, and z direction
u_0, θ	Axial displacement and rotation of mid-plane
λ	Power index
F	Auxiliary function
t	Knot vectors
$n+1$	Number of control points
k	order of the basis function
B	Position vector of control points
k_s	Shear correction factor
$N_{i,k}(t)$	B-spline basis function
$\varepsilon_{xx}, \gamma_{xz}$	Normal strain and shear strain
σ_{xx}, τ_{xz}	Normal stress and Shear stress

δU_0	Internal Strain Energy
δU_R	Work done due to centrifugal force
δU_P	Work done due to uniformly distri–buted load by *'q'*
N_{xx}, M_{xx}	Normal force, Bending moment.
Q	shear force
N_R	Centrifugal Force

СТАТИЧКО ПОНАШАЊЕ ФУНКЦИОНАЛНО СТЕПЕНОВАНИХ РОТИРАЈУЋИХ КОНЗОЛНИХ ГРЕДА КОРИШЋЕЊЕМ Б-СПЛАЈН ТЕХНИКЕ КОЛОКАЦИЈЕ

Ш. Чичкеде, Д. Махапатра, Ш. Санјал, Ш. Бомвик

Овај рад извештава о статичком понашању функ–ционално степеноване ротирајуће греде на основу Тимошенкове теорије греде, која укључује ефекат смичне деформације. Принцип виртуелног поме–рања се примењује да би се извела главна једначина за функционално степенасту (ФГ) ротирајућу греду, с обзиром на ефекат центрифугалног укрућења. Техника колокације Б-сплајн се користи за решавање диференцијалне једначине, а својства материјала су функција дистрибуције закона степена.

Утицај индекса снаге материјала и брзине ротације на статичке карактеристике функционално степе–нованих ротирајућих конзолних греда испитан је за два различита односа виткости. Добијени резултати показују угиб греде и нормалне и смичне напоне греде за вредности градијента снаге и брзине ротације. Резултати помажу да се закључи да се градација материјала може искористити за побољшање функционисања ротирајућих структура као што су ротор хеликоптера, пропелери авиона, лопатице ветрењаче итд.